Unconventional Robust Spin-Transfer Torque in Noncollinear Antiferromagnetic Junctions

Srikrishna Ghosh,[1] Aurelien Manchon,[2] and Jakub Železný[1]
[1]Institute of Physics, Czech Academy of Sciences, Cukrovarnická 10, 162 00 Praha 6, Czech Republic
[2]CINaM, Aix-Marseille Université, CNRS, Marseille, France

(Received 3 September 2021; revised 25 November 2021; accepted 13 January 2022; published 4 March 2022; corrected 9 June 2022)

Ferromagnetic spin valves and tunneling junctions are crucial for spintronics applications and are one of the most fundamental spintronics devices. Motivated by the potential unique advantages of antiferromagnets for spintronics, we theoretically study here junctions built out of noncollinear antiferromagnets. We demonstrate a large and robust magnetoresistance and spin-transfer torque capable of ultrafast switching between parallel and antiparallel states of the junction. In addition, we show that a new type of self-generated torque appears in the noncollinear junctions.

DOI: 10.1103/PhysRevLett.128.097702

In ferromagnetic materials, the spins of electrons that carry electrical current are preferentially oriented along the magnetization direction: the electrical current is spin polarized. When this spin-polarized current is injected into a second ferromagnet (FM) with a misaligned magnetization orientation, the spin polarization has to reorient along this new magnetization direction. Because of angular momentum conservation, this reorientation exerts a torque on the FM, known as the spin-transfer torque (STT) [1,2]. This torque can be used to switch magnetization in a FM or to move magnetic domain walls. It is typically utilized in nanoscopic devices composed of two thin ferromagnetic layers separated by a metallic or insulating spacer and whose relative orientation is detected via the giant (GMR) or tunneling magnetoresistance. It is at the basis of the magnetic random access memories [3].

In recent years, attention has been drawn to magnetic materials with a local magnetic order but no net magnetic moment, referred to as antiferromagnets (AFMs). AFMs offer significant advantages over FMs for spintronics applications [4–7]. Their magnetic dynamics is several orders of magnitude faster than FMs, allowing for much faster switching. The lack of a net magnetic moment implies no stray field, thus possibly allowing for closer packing of individual bits. Furthermore, a large variety of antiferromagnetic materials exists, such as insulators and semiconductors, multiferroics [8], or superconductors [9] (see also [10]). FM materials accommodating such exotic electronic properties are much less common in nature. A number of theoretical works have shown that the STT, as well as GMR, can also exist in AFM junctions [7,11–14]. In contrast to the FM case, however, such effects arise from quantum-coherent scattering [11] and, as a result, are very sensitive to the presence of disorder [7,15–17]. This lack of robustness has a fundamental reason: in the simple high-symmetry AFMs that were primarily studied, the electrical current is not spin polarized and, consequently, the STT has to vanish in the semiclassical limit [17]. It was found, however, that in the tunneling case STT can be more robust [18], although the reasons for this are not fully understood. Experimentally, no clear evidence of STT in an AFM junction has been found so far [7]. Instead, AFM spintronics has mainly focused on relativistic effects and, in particular, on spin-orbit torques [19], exploiting the large spin-orbit coupling provided by the presence of heavy metals, either in the magnetic unit cell [20,21] or as an adjacent layer, the latter acting as a source of spin Hall effect [22]. Nonetheless, no equivalent to STT in FMs has been realized to date due to the difficulty to achieve semiclassical spin-polarized current out of AFMs.

Recently though, it was discovered that, in some types of AFMs, such spin-polarized currents can exist. This was first found for noncollinear AFMs (AFMs in which the individual moments are not oriented along a single axis), such as Mn_3Ir or Mn_3Sn [23,24], but later also found to exist in collinear AFMs such as RuO_2 [25–30]. These spin-polarized currents are directly analogous to the spin-polarized currents in FMs. As a matter of fact, like in FMs, these currents are extrinsic, i.e., driven by intraband transitions of the Fermi surface electrons, their polarization is aligned along a direction set by the relative orientation of the charge flow and the AFM texture, and, most importantly, they are robust against momentum scattering. These properties suggest that a robust STT, as well as magnetoresistive effects, could exist in junctions composed of AFMs in which the spin-polarized current exists [23,31,32].

In this Letter, using tight-binding numerical simulations, we demonstrate that these spin-polarized currents can drive magnetoresistance and STT in noncollinear AFM junctions, displaying striking differences compared to their FM counterparts. We consider a relatively simple 2D model, which is not meant to quantitatively describe realistic systems but which covers the most important features of noncollinear

coplanar antiferromagnets of interest to experiments (for example Mn_3Ir or Mn_3Sn). Importantly, this model allows for a comprehensive study of the role of disorder, a crucial ingredient that destroys quantum coherence and quenches STT in collinear AFM junctions [11,16]. We show that the STT survives in the presence of point defects, but also structural imperfections, which invariably exist in real systems but have been disregarded until now. Our numerical results show that the STT in noncollinear AFM junctions originates from the absorption of the spin-polarized current generated in *both* AFM layers, as illustrated in Fig. 1. As a consequence, we find that apart from the conventional STT a new type of torque appears in the noncollinear AFMs, which does not exist in FMs. Unlike the conventional STT, this torque does not originate from a spin transfer between the two magnetic layers but rather is local and self-induced. Furthermore, because of the unconventional noncollinear magnetic ordering, the torque is present for any relative orientation of the two AFM layers. This observation sharply contrasts with what is usually observed in FM junctions, where the STT vanishes for the parallel or antiparallel configurations, which implies that thermal fluctuations are required to assist the magnetization switching, resulting in stochasticity and slower reversal time. Our simulations of STT-induced dynamics in the AFM junctions show deterministic switching on a picosecond timescale.

We consider a 2D AFM system, shown in Fig. 1(a). The system is hexagonal with three atoms in a unit cell; however, for easy construction of the junctions, we double the unit cell, which makes the unit cell rectangular. Similar magnetic order exists in real materials, such as the Mn_3X AFMs [23,33,34]. The model we use consists of conduction s electrons coupled to on-site magnetic moments. This model has been utilized in previous studies of noncollinear AFMs [35–37]. We do not include spin-orbit coupling in our model, since the aim is to explore nonrelativistic effects, in analogy to the FM junctions, where the dominant effects are nonrelativistic in origin. Furthermore, previous calculations of spin-polarized currents in Mn_3X AFMs showed only a weak dependence on spin-orbit coupling [23]. In absence of disorder, the system is described by the following Hamiltonian:

$$H = t\sum_{\langle ab\rangle\alpha} c^{\dagger}_{a\alpha}c_{b\alpha} + J\sum_{a\alpha,\beta}(\boldsymbol{\sigma}\cdot\mathbf{m}_a)_{\alpha\beta}c^{\dagger}_{a\alpha}c_{a\beta}. \quad (1)$$

Here, $c^{\dagger}$ and c denote the creation and annihilation operators, respectively, a and b denote the site index, and α and β denote the spin index. The first term is the nearest-neighbor hopping term, with t representing the hopping magnitude. The second term represents the coupling of the conduction electrons to the on-site magnetic moments. Here $\mathbf{m}_a$ is the magnetic moment direction, J is the exchange parameter, and $\boldsymbol{\sigma}$ is the vector of Pauli matrices. We always set $t = 1$ and $J = -1.7$ eV.

To describe disorder, we include for each site on-site energy chosen randomly from a Gaussian distribution centered at zero and with a standard deviation D. We describe the quantum transport using the scattering (Landauer-Büttiker) formalism as implemented in the KWANT package [38]. We consider a system composed of two magnetic layers separated by a nonmagnetic spacer (scattering region) and attach to the system perfectly periodic semi-infinite leads as illustrated in Fig. 1(b). The transport properties of the system are described by scattering of the incoming states from the left lead to the outgoing states in the left and right leads.

For simplicity, we consider the same magnetic order in the left and right leads as for the left and right magnetic layers, respectively, as illustrated in Fig. 1(b). We note that the leads are perfectly periodic, whereas the magnetic layers within the scattering region contain disorder. For completeness, we also discuss in the Supplemental Material [39] calculation with nonmagnetic leads, which physically correspond to thin magnetic layers. In general, we find that for the FM junctions the results for nonmagnetic leads are very similar, whereas for the noncollinear AFM there can be significant differences, but the qualitative behavior is still generally the same. We always set the width of the magnetic layers and the spacer along the x direction to five unit cells each. The width of the system along the y direction is set to 50 unit cells, which ensures that the effect of the top and bottom interfaces is negligible. To describe interface roughness, we randomly include atomic interfacial steps using a random walk along the interfaces between the magnetic leads and the spacer as described in the Supplemental Material [39]. The magnitude of the interfacial disorder is controlled by the parameter n_{steps}, which determines the average number of the interfacial steps.

Within the scattering formalism, the transport is due to the difference of the chemical potentials of the left and the right leads $\delta\mu$. For the case of the electric effects, this difference is due to applied voltage V: $\delta\mu = -eV$. We always assume transport from the left to the right and also assume that the voltage is small, i.e., we will assume that

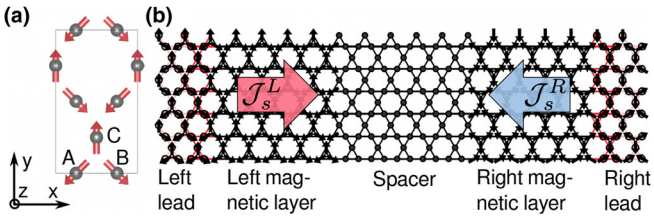

FIG. 1. (a) The unit cell of the model. (b) Illustration of the junction. The left and right leads are periodic and semi-infinite along the x directions. The junction is finite along the y direction. In the calculation, the width along y is much wider than illustrated here. When a charge current is injected through the junction, a spin current $\mathcal{J}_s^{L(R)}$ builds up in the left (right) AFM electrode. The former induces a conventional STT on the right AFM, while the latter is at the origin of the self-induced STT.

the response to the electric field is linear. The current induced by the voltage is given by $I = GV$, where $G = (e^2/h)\sum_{nm}|t_{nm}|^2$ and t_{nm} is the transmission amplitude from incoming state n in the left lead to outgoing state m in the right lead. Using the scattering wave functions ψ_n inside the lead associated with the n incoming states of the left lead at energy E_F, we can evaluate response of any quantity. For an observable A represented by operator $\hat{A}$ we have $\delta A = \chi_A \delta\mu$, where $\chi_A = \sum_n \langle\psi_n|\hat{A}|\psi_n\rangle$. Note that we assume here a zero temperature Fermi-Dirac distribution. We are primarily interested in the torque. The torque acting on a site a can be calculated using the torque operator $\hat{\mathbf{T}}_a = -J\sum_{\alpha\beta}(\mathbf{m}_a \times \boldsymbol{\sigma})_{\alpha\beta} c^\dagger_{a\alpha} c_{a\beta}$. As we discuss in the Supplemental Material [39], the torque can also be evaluated from the nonequilibrium spin accumulation and, since we do not consider spin-orbit coupling, the torque is also directly related to spin current: the torque on a site is given by the spin source at this site. We note that, although the spin of the conduction electrons is strongly nonconserved in the noncollinear systems, spin current is nevertheless well defined in the nonrelativistic limit since there is no conversion of the spin angular momentum to orbital angular momentum.

In Fig. 2(b), we give the calculated torque in the right magnetic layer for FM and AFM junctions as a function of the rotation of the right magnetic layer in the x–y plane. Here we set $D = 0.2$ eV and $n_{\text{steps}} = 25$. In the FM case, the torque at the right magnetic layer originates from the absorption of the spin-polarized current from the left magnetic layer. In the FMs, only the component of the spin perpendicular to the magnetization is efficiently absorbed.

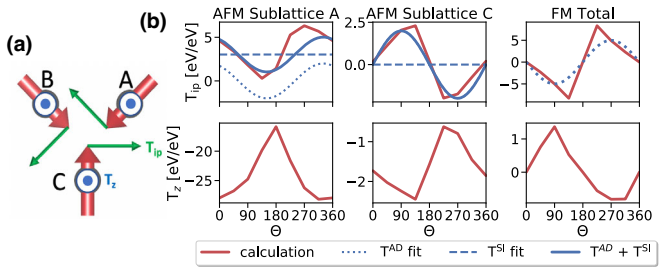

FIG. 2. (a) The decomposition of the torque into in-plane and T_z components. (b) The dependence of the torque in the right magnetic layer on the rotation of the right magnetic layer in the x–y plane for the AFM and FM junctions. For the FM junction we show the total torque; for the AFM junction we show a sublattice projected torque. Since sublattice B is very similar to sublattice A, we only show the sublattice A here and give sublattice B in the Supplemental Material [39]. Here $\theta = 0°, 90°, 180°$ correspond to the parallel, perpendicular, and antiparallel configurations of the junctions, respectively (see Fig. 3). The in-plane component of the torque is fitted by the combination of $\mathbf{T}^{\text{SI}}$ and $\mathbf{T}^{\text{AD}}$. Here $E_F = -1.25$ eV, $D = 0.2$ eV, and $n_{\text{steps}} = 25$. The torque has units of eV as is given per the applied bias, which is also given in units of eV.

Since the torque is directly given by the absorbed spin current, we have, assuming a full absorption of the perpendicular component: $\mathbf{T}_R \sim \mathbf{m}_L - (\mathbf{m}_L \cdot \mathbf{m}_R)\mathbf{m}_R = \mathbf{m}_R \times (\mathbf{m}_L \times \mathbf{m}_R)$. This is the well-known antidamping torque. As shown in Fig. 2(b), the antidamping torque is the dominant term in our calculations.

In FMs the right magnetic layer also generates a spin-polarized current; however, this spin current does not create a torque in the right magnetic layer since it is polarized along its magnetization. Thus, the torque in the right magnetic layer is due to a spin-polarized current from the left magnetic layer and vice versa. In the noncollinear AFMs, the situation is different. Because of the noncollinearity, the spin-polarized current from the right magnetic layer can also be absorbed in the right magnetic layer (and analogously for the left) since some sublattices will always have magnetization misaligned with the spin polarization. As a consequence, a torque is present even in a junction containing only one magnetic layer, as illustrated in Fig. 3(a). The torque in the noncollinear AFMs thus has two sources: a spin-transfer torque due to the other magnetic layer and a local, self-induced torque due to spin-polarized current from the layer itself. For the configuration given in Fig. 1, the spin polarization of the spin current is constrained by symmetry to lie along the y direction [23], which also happens to be the direction of the C sublattice. In the nonrelativistic limit, any rotation of the magnetic order will result in the same rotation of the spin polarization, and thus the spin polarization will always be oriented along the $\mathbf{m}_C$ direction. Assuming absorption of the perpendicular component on each sublattice will thus lead to torques in the right magnetic layer: an antidamping (AD) torque $\mathbf{T}^{\text{AD}}_{R,a} \sim \mathbf{m}_{R,a} \times (\mathbf{m}_{L,C} \times \mathbf{m}_{R,a})$ and self-induced (SI) torque $\mathbf{T}^{\text{SI}}_{R,a} \sim \mathbf{m}_{R,a} \times (\mathbf{m}_{R,C} \times \mathbf{m}_{R,a})$ (here a denotes the sublattice). As shown in Fig. 2(b) we find that our calculations are indeed well described by the combination of the antidamping torque and the self-induced torque (see Supplemental Material [39] for calculations with different parameters).

In addition to the in-plane torque, which is well described by the combination of $\mathbf{T}^{\text{AD}}$ and $\mathbf{T}^{\text{SI}}$, we also find a T_z component of the torque. In FMs this torque typically has a fieldlike character, which we also find here. This torque occurs because the spin current that is reflected from the right magnetic layer contains a z-polarized component when the two magnetic layers are misaligned. In the AFM junctions, this torque also appears. As shown in the Supplemental Material [39], we find that it can be very large on individual sublattices, but when summed up tends to be smaller than the in-plane component.

The connection between the spin-polarized current and the torque is illustrated in Fig. 3, where we show the spin current and the total torque within the junction as a function of the x coordinate. We see that for all the configurations of the junction the torque is directly connected to absorption or generation of the spin-polarized current. In the FM case, no

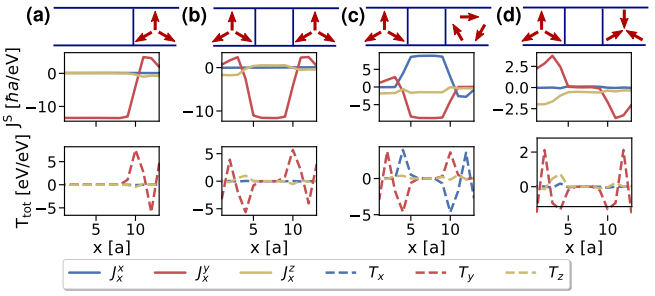

FIG. 3. The spin current and torque as a function of the x coordinate (a denotes the lattice constant along the x direction) for (a) junction composed of only a nonmagnetic and one magnetic layer, (b) parallel, (c) perpendicular, and (d) antiparallel configurations of the AFM junction. We sum up both the torque and the spin current within each unit cell and then sum up also along the y direction. J_x^i denote spin current flowing along the x direction with spin polarization along i. We set $D = 0.2$ eV, $n_{\text{steps}} = 25$, and $E_F = -1.25$ eV.

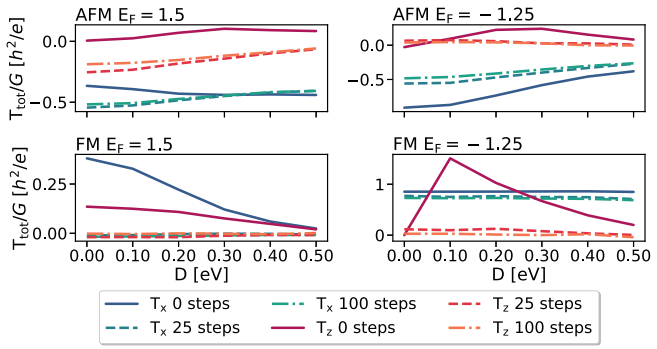

FIG. 4. The dependence of the torque magnitude scaled by the conductance on the disorder parameter D and on the interfacial disorder characterized by number of interfacial steps for the FM and AFM junction and for two values of E_F. The T_y component is not shown here since it has a similar dependence on magnitude as T_x. For T_z we set $\theta = 90°$; for T_x, $\theta = 135°$ for the FM and $\theta = 90°$ for the AFM.

torque or, equivalently, no spin source can be present in the parallel or antiparallel configurations of the junction or in a junction containing only one FM layer, since in such a case spin is conserved. In contrast, in the noncollinear case, we find a nonvanishing torque in any configuration because in the noncollinear AFM spin is never conserved. In the parallel and antiparallel cases, both $\mathbf{T}^{\text{SI}}$ and $\mathbf{T}^{\text{AD}}$ contribute since in the noncollinear system $\mathbf{T}^{\text{AD}}$ is nonzero for some sublattices for any orientation of the junction and will always sum up to nonzero total torque. We note that, in addition to the torque due to a global spin current illustrated in Fig. 3, also a torque due to local spin currents can occur. This is the case of the large T_z torque for the A sublattice illustrated in Fig. 2(b).

We use the calculated torque to simulate switching of the AFM junction. As discussed in the Supplemental Material [39], we find that both the in-plane torque characterized by a combination of $\mathbf{T}^{\text{SI}}$ and $\mathbf{T}^{\text{AD}}$, as well as the T_z torque, can deterministically switch the junction between parallel and antiparallel states using current pulses with opposite directions. Crucially, the switching is ultrafast (on a picosecond timescale), since in AFMs the dynamics is enhanced by the exchange interaction. This comes into play since the torque initially slightly cants the magnetic moments, which results in a large exchange torque. Unlike in the FM case, where thermal activation is necessary to activate the switching, since no torque exists in the parallel state or antiparallel states, we find that in the AFM case switching is possible directly from the parallel or antiparallel states since the torque is always present. We note that $\mathbf{T}^{\text{SI}}$, which is typically the dominant term in our calculations, cannot by itself be used for deterministic switching. This is because this torque is nonrelativistic and internally generated, which means that when the magnetic order is rotated the torque is rotated in the same way and can thus never vanish. As a result, the other magnetic layer is crucial here. Our simulations show that when $\mathbf{T}^{\text{SI}}$ is combined with $\mathbf{T}^{\text{AD}}$, deterministic switching is possible and that the $\mathbf{T}^{\text{SI}}$ can reduce the $\mathbf{T}^{\text{AD}}$ necessary for switching. The $\mathbf{T}^{\text{SI}}$ torque could also be used for spin-torque oscillators.

In Fig. 4(a), we show the dependence of the torque magnitude on the on-site and interfacial disorder for the FM and AFM junctions. For simplicity, we give here the dependence for the total torque; however, the conclusions are generally the same when the sublattice torque is considered. We give the results here for two values of the Fermi level and we also scale the torque by the conductance since the torque magnitude per current density is the main quantity for practical utilization of the torque. Overall, we find that the torque in the AFM junctions has a similar magnitude and robustness against disorder as in the FM junctions. In agreement with previous considerations, we find that the interfacial steps reduce strongly the T_z component of the torque; in contrast, the T_x and T_y components are more robust and survive even with significant interfacial disorder present. We also find no strong reduction of the torque magnitude with the disorder parameter D. We note that the case of FM with $E_F = 1.5$ eV is somewhat an exception, as we find that in this case the torque is more sensitive to disorder than in the other cases. As shown in the Supplemental Material [39], the angular dependence of the torque is also generally unchanged with the disorder. In the Supplemental Material [39], we show the dependence of GMR on disorder for the FM and AFM junctions. We find that in both cases the GMR is strongly reduced by disorder, but non-negligible GMR is present even in the presence of significant disorder. Crucially, the robustness of the GMR is similar in the AFM as in the FM.

We acknowledge the Grant Agency of the Czech Republic Grant No. 19-18623Y, Ministry of Education of the Czech Republic Grant No. LM2018110, EU FET

Open RIA Grant No. 766566, and support from the Institute of Physics of the Czech Academy of Sciences and the Max Planck Society through the Max Planck Partner Group Programme. This work was supported by the Ministry of Education, Youth and Sports of the Czech Republic through the e-INFRA CZ (ID:90140). A. M. acknowledges support from the Excellence Initiative of Aix-Marseille Université—A*Midex, a French "Investissements d'Avenir" program.

[1] A. Brataas, A. D. Kent, and H. Ohno, Current-induced torques in magnetic materials, Nat. Mater. **11**, 372 EP (2012).
[2] D. Ralph and M. Stiles, Spin transfer torques, J. Magn. Magn. Matter. **320**, 1190 (2008).
[3] D. Apalkov, B. Dieny, and J. M. Slaughter, Magnetoresistive random access memory, Proc. IEEE **104**, 1796 (2016).
[4] T. Jungwirth, X. Marti, P. Wadley, and J. Wunderlich, Antiferromagnetic spintronics, Nat. Nanotechnol. **11**, 231 (2016).
[5] V. Baltz, A. Manchon, M. Tsoi, T. Moriyama, T. Ono, and Y. Tserkovnyak, Antiferromagnetic spintronics, Rev. Mod. Phys. **90**, 015005 (2018).
[6] T. Jungwirth, J. Sinova, A. Manchon, X. Marti, J. Wunderlich, and C. Felser, The multiple directions of antiferromagnetic spintronics, Nat. Phys. **14**, 200 (2018).
[7] J. Železný, P. Wadley, K. Olejník, A. Hoffmann, and H. Ohno, Spin-transport, spin-torque and memory in antiferromagnetic devices, Nat. Phys. **14**, 220 (2018).
[8] W. Eerenstein, N. D. Mathur, and J. F. Scott, Multiferroic and magnetoelectric materials, Nature (London) **442**, 759 (2006).
[9] X. F. Lu, N. Z. Wang, H. Wu, Y. P. Wu, D. Zhao, X. Z. Zeng, X. G. Luo, T. Wu, W. Bao, G. H. Zhang, F. Q. Huang, Q. Z. Huang, and X. H. Chen, Coexistence of superconductivity and antiferromagnetism in $(Li_{0.8}Fe_{0.2})$OHFeSe, Nat. Mater. **14**, 325 (2015).
[10] V. Bonbien, F. Zhuo, A. Salimath, O. Ly, A. Abbout, and A. Manchon, Topological aspects of antiferromagnets, J. Phys. D **55**, 103002 (2022).
[11] A. S. Núñez, R. A. Duine, P. Haney, and A. H. MacDonald, Theory of spin torques and giant magnetoresistance in antiferromagnetic metals, Phys. Rev. B **73**, 214426 (2006).
[12] P. M. Haney, D. Waldron, R. A. Duine, A. Núñez, H. Guo, and A. H. MacDonald, *Ab initio* giant magnetoresistance and current-induced torques in Cr/Au/Cr multilayers, Phys. Rev. B **75**, 174428 (2007).
[13] P. Merodio, A. Kalitsov, H. B ea, V. Baltz, and M. Chshiev, Spin-dependent transport in antiferromagnetic tunnel junctions, Appl. Phys. Lett. **105**, 122403 (2014).
[14] M. Stamenova, R. Mohebbi, J. Seyed-Yazdi, I. Rungger, and S. Sanvito, First-principles spin-transfer torque in CuMnAs|GaP|CuMnAs junctions, Phys. Rev. B **95**, 060403(R) (2017).
[15] R. A. Duine, P. M. Haney, A. S. Núñez, and A. H. MacDonald, Inelastic scattering in ferromagnetic and antiferromagnetic spin valves, Phys. Rev. B **75**, 014433 (2007).
[16] Hamed Ben Mohamed Saidaoui, A. Manchon, and X. Waintal, Spin transfer torque in antiferromagnetic spin valves: From clean to disordered regimes, Phys. Rev. B **89**, 174430 (2014).
[17] A. Manchon, Spin diffusion and torques in disordered antiferromagnets, J. Phys. Condens. Matter **29**, 104002 (2017).
[18] Hamed Ben Mohamed Saidaoui, X. Waintal, and A. Manchon, Robust spin transfer torque in antiferromagnetic tunnel junctions, Phys. Rev. B **95**, 134424 (2017).
[19] A. Manchon, J. Železný, I. M. Miron, T. Jungwirth, J. Sinova, A. Thiaville, K. Garello, and P. Gambardella, Current-induced spin-orbit torques in ferromagnetic and antiferromagnetic systems, Rev. Mod. Phys. **91**, 035004 (2019).
[20] J. Železný, H. Gao, K. Výborný, J. Zemen, J. Mašek, A. Manchon, J. Wunderlich, J. Sinova, and T. Jungwirth, Relativistic Néel-Order Fields Induced by Electrical Current in Antiferromagnets, Phys. Rev. Lett. **113**, 157201 (2014).
[21] P. Wadley *et al.*, Electrical switching of an antiferromagnet, Science **351**, 587 (2016).
[22] X. Z. Chen, R. Zarzuela, J. Zhang, C. Song, X. F. Zhou, G. Y. Shi, F. Li, H. A. Zhou, W. J. Jiang, F. Pan, and Y. Tserkovnyak, Antidamping-Torque-Induced Switching in Biaxial Antiferromagnetic Insulators, Phys. Rev. Lett. **120**, 207204 (2018).
[23] J. Železný, Y. Zhang, C. Felser, and B. Yan, Spin-Polarized Current in Noncollinear Antiferromagnets, Phys. Rev. Lett. **119**, 187204 (2017).
[24] G. Gurung, D.-F. Shao, and E. Y. Tsymbal, Transport spin polarization of noncollinear antiferromagnetic antiperovskites, Phys. Rev. Mater. **5**, 124411 (2021).
[25] M. Naka, S. Hayami, H. Kusunose, Y. Yanagi, Y. Motome, and H. Seo, Spin current generation in organic antiferromagnets, Nat. Commun. **10**, 4305 (2019).
[26] R. González-Hernández, L. Šmejkal, K. Výborný, Y. Yahagi, J. Sinova, T. c. v. Jungwirth, and J. Železný, Efficient Electrical Spin Splitter Based on Nonrelativistic Collinear Antiferromagnetism, Phys. Rev. Lett. **126**, 127701 (2021).
[27] K.-H. Ahn, A. Hariki, K.-W. Lee, and J. Kuneš, Antiferromagnetism in ruo_2 as d-wave Pomeranchuk instability, Phys. Rev. B **99**, 184432 (2019).
[28] S. Hayami, Y. Yanagi, and H. Kusunose, Momentum-dependent spin splitting by collinear antiferromagnetic ordering, J. Phys. Soc. Jpn. **88**, 123702 (2019).
[29] L. Šmejkal, R. González-Hernández, T. Jungwirth, and J. Sinova, Crystal time-reversal symmetry breaking and spontaneous Hall effect in collinear antiferromagnets, Sci. Adv. **6**, eaaz8809 (2020),
[30] L.-D. Yuan, Z. Wang, J.-W. Luo, E. I. Rashba, and A. Zunger, Giant momentum-dependent spin splitting in centrosymmetric low-Z antiferromagnets, Phys. Rev. B **102**, 014422 (2020).
[31] D.-F. Shao, S.-H. Zhang, M. Li, C.-B. Eom, and E. Y. Tsymbal, Spin-neutral currents for spintronics, Nat. Commun. **12**, 7061 (2021).
[32] L. Šmejkal, A. B. Hellenes, R. González-Hernández, J. Sinova, and T. Jungwirth, Giant and Tunneling Magnetoresistance in Unconventional Collinear Antiferromagnets

with Nonrelativistic Spin-Momentum Coupling, Phys. Rev. X **12**, 011028 (2022).
[33] S. Tomiyoshi and Y. Yamaguchi, Magnetic structure and weak ferromagnetism of Mn3Sn studied by polarized neutron diffraction, J. Phys. Soc. Jpn. **51**, 2478 (1982).
[34] T. Yamaoka, Antiferromagnetism in γ-phase mn-ir alloys, J. Phys. Soc. Jpn. **36**, 445 (1974).
[35] H. Chen, Q. Niu, and A. H. MacDonald, Anomalous Hall Effect Arising from Noncollinear Antiferromagnetism, Phys. Rev. Lett. **112**, 017205 (2014).
[36] Y. Zhang, J. Železný, Y. Sun, J. van den Brink, and B. Yan, Spin Hall effect emerging from a noncollinear magnetic lattice without spin-orbit coupling, New J. Phys. **20**, 073028 (2018).
[37] S. Hayami, Y. Yanagi, and H. Kusunose, Spontaneous antisymmetric spin splitting in noncollinear antiferromagnets without spin-orbit coupling, Phys. Rev. B **101**, 220403(R) (2020).
[38] C. W. Groth, M. Wimmer, A. R. Akhmerov, and X. Waintal, KWANT: A software package for quantum transport, New J. Phys. **16**, 063065 (2014).
[39] See Supplemental Material at http://link.aps.org/supplemental/10.1103/PhysRevLett.128.097702 for derivation of the expression for the spin-orbit torque, simulation of switching, and additional calculation, which includes Refs. [40–44].
[40] P. Gambardella and I. M. Miron, Current-induced spin-orbit torques, Phil. Trans. R. Soc. A **369**, 3175 (2011).
[41] J. Shi, P. Zhang, D. Xiao, and Q. Niu, Proper Definition of Spin Current in Spin-Orbit Coupled Systems, Phys. Rev. Lett. **96**, 076604 (2006).
[42] T. Gilbert, Classics in magnetics a phenomenological theory of damping in ferromagnetic materials, IEEE Trans. Magn. **40**, 3443 (2004).
[43] J. Železný, Macrospin LLG, https://bitbucket.org/zeleznyj/macrospin-llg.
[44] H. V. Gomonay, R. V. Kunitsyn, and V. M. Loktev, Symmetry and the macroscopic dynamics of antiferromagnetic materials in the presence of spin-polarized current, Phys. Rev. B **85**, 134446 (2012).

Correction: The lower panel of the previously published Fig. 3 was positioned improperly and has been fixed.